Thermochimica Acta 519 (2011) 59–64

Contents lists available at ScienceDirect

Thermochimica Acta

journal homepage: www.elsevier.com/locate/tca

Effect of heating rate and sample geometry on the apparent specific heat capacity: DSC applications

T. Kousksou[a,*], A. Jamil[b], K. El Omari[a], Y. Zeraouli[a], Y. Le Guer[a]

[a] Laboratoire des Sciences de l'Ingénieur Appliquées à la Mécanique et au Génie Electrique (SIAME), Université de Pau et des Pays de l'Adour – IFR – A. Jules Ferry, 64000 Pau, France
[b] École Supérieure de Technologie de Fès, Université Sidi Mohamed Ibn Abdelah, Route d'Imouzzer BP 2427, Morocco

ARTICLE INFO

Article history:
Received 30 November 2010
Received in revised form 16 February 2011
Accepted 17 February 2011
Available online 2 March 2011

Keywords:
Heat transfer
PCM
Specific heat capacity
DSC
Melting
Enthalpic method

ABSTRACT

Differential scanning calorimetry (DSC) and numerical simulations have been used to determine some kinetics parameters of phase change materials (PCM). The heating rate affects the development of the DSC thermograms and also the apparent specific heat capacity of the PCM during the phase change process. PCM geometry has also a definitive influence on the DSC thermograms and on the apparent specific heat capacity but seems to have no effect on the latent heat energy calculations.

1. Introduction

Thermal energy storage (TES) is very important in many energy systems [1–3]. The advantages of using TES systems are to balance the energy supply and demand, or to collect energy irregularly generated like solar energy for late use.

The development history of latent storage systems is the development history of storage materials. Among the most extensive references related with phase change materials (PCMs), one can cite Abhat et al. [4], Husnain [5], Dincer [6], Mohammed et al. [7], Felix Regin et al. [1] and Zalba et al. [8]. These contain a complete review of the type of materials that have been used, their classification, characteristics, advantages and disadvantages and the various experimental techniques used to determine the behavior of these materials during melting and solidification processes.

Phase change materials (PCM) are thermal storage materials with a high storage density for small temperature range application. The design of a thermal storage system within this narrow temperature range has to be founded on reliable and high resolution material data. The accurate determination of the PCM's heat storage capability as a function of temperature is crucial.

DSC is one of the most widely used analytical instruments because of the ease with which it can provide large amounts of thermodynamic data [9]. From a single DSC test that consists in regularly cooling down and heating of a sample, it is expected to obtain qualitative and quantitative information on the phase transitions of a sample, such as transition temperature, enthalpy, thermal conductivity, heat capacity, specific heat, and latent heat [10–14]. The accuracy of DSC measurements of standard materials is discussed in detail by Richardson [15] and Rudtsh [16]. Concerning DSC measurements of PCM, the accuracy of the measurement is dominated by the heating and sample size.

The purpose of this work is to illustrate the effect of heating rate and sample geometry on the apparent specific heat capacity of the PCM samples.

2. Experimental

Thermal analysis was carried out using a PYRIS DIAMOND DSC of PerkinElmer. The temperature scale of the instrument was carefully calibrated by the melting point of pure ice (273.15 K or 0 °C) and mercury (234.32 K or −38.82 °C). The principle of the power-compensation used in the present study is widely detailed in Refs. [9,17]. We have already presented the experimental cell in Ref. [17], which consists of a cylindrical cell of height $Z_0 = 1.1$ mm and radius $R = 2.215$ mm (Fig. 1).

* Corresponding author.
E-mail address: Tarik.kousksou@univ-pau.fr (T. Kousksou).

0040-6031/$ – see front matter © 2011 Elsevier B.V. All rights reserved.
doi:10.1016/j.tca.2011.02.033

Nomenclature

c_p	specific heat capacity ($J\,kg^{-1}\,K^{-1}$)
c_R	specific heat capacity of the reference cell ($J\,kg^{-1}\,K^{-1}$)
ΔA	area (m^2)
L_F	latent heat of ice melting ($J\,kg^{-1}$)
M	mass (kg)
R	cell radius (m)
t	time (s)
T	temperature (K)
T_0	initial temperature (K)
$U_{1,2}$	heat transfer coefficient ($W\,m^{-2}\,K^{-1}$)
V	volume (m^3)
X	liquid fraction
Z	cell height (m)

Greek letters

β	heating rate ($K\,min^{-1}$)
λ	heat conductivity ($W\,m^{-1}\,K^{-1}$)
ρ	mass density ($kg\,m^{-3}$)
φ	specific heat flow rate ($W\,kg^{-1}$)

Subscripts

l	liquid
s	solid

The apparatus gives the energy flux Φ the difference between the heat powers maintaining the plate supporting the active cell containing the PCM and the plate supporting the reference cell

$$\Phi = \Phi_{\text{active cell}} - \Phi_{\text{reference cell}} \tag{1}$$

As indicated in Ref. [17], the power exchanged at the reference plate is practically constant and equal to $\Phi_{\text{reference cell}} = \beta c_R$ where c_R is the specific heat of the reference cell and β is the heating rate. So to simplify the model we will omit the second term from the calculation of Φ.

The DSC experiments were conducted by placing approximately 6–10 mg of each PCM in a standard aluminum DSC sample pan. The sample was cooled at 5 °C/min from 4 °C, until crystallization of the PCM (observed as a sharp negative peak on the DSC thermogram) typically between −30 and −40 °C. The sample was then re-equilibrated at this temperature for 3–5 min. Isothermal equilibrium at this temperature will permit the ice crystals to exist but not grow. The sample was then heated from −40 °C to 25 °C using different heating rates, to obtain the magnitude and the temperature dependence of the heat absorbed (i.e. the thermogram).

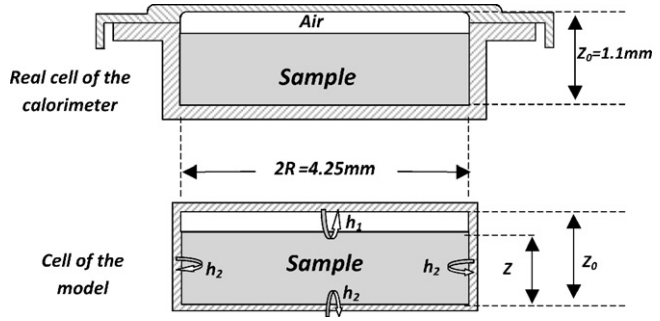

Fig. 1. Cell-A.

3. Physical model

The model which we have adopted to describe the thermal transfers during the phase shift of the studied solution is based on an enthalpic formulation proposed by Voller and his co-workers [18,19]. This formulation rests on the partition of the volume occupied by the solution into a finite number of control volumes and the handwriting the energy conservation in cylindrical coordinates:

$$\rho c_p \frac{\partial T}{\partial t} = \lambda \left(\frac{\partial^2 T}{\partial r^2} + \frac{1}{r}\frac{\partial T}{\partial r} + \frac{\partial^2 T}{\partial z^2} \right) + \rho_s \Delta H \frac{\partial X}{\partial t} \tag{2}$$

where ρ, c_p and λ indicate, respectively, the mass density, the specific heat capacity and the heat conductivity of the PCM. X indicates the liquid fraction in the DSC cell. The coefficient ΔH is the latent heat of melting. During the melting process, the sample is regarded as a homogeneous material whose physical properties depend on the liquid fraction.

To take into account the air between the solution and the cover of the cell, we consider two different heat exchange coefficients U_1 and U_2. So, the boundaries conditions are:

$$\left(\frac{\partial T}{\partial r}\right)_{r=0} = 0 \tag{3}$$

$$-\lambda \left(\frac{\partial T}{\partial r}\right)_{r=R} = U_2 (T - T_{\text{plt}}) \tag{4}$$

$$-\lambda \left(\frac{\partial T}{\partial z}\right)_{z=0} = U_2 (T - T_{\text{plt}}) \tag{5}$$

$$-\lambda \left(\frac{\partial T}{\partial z}\right)_{z=Z} = U_1 (T - T_{\text{plt}}) \tag{6}$$

where T_{plt} is the plates temperature and it is programmed to be linear function.

$$T_{\text{plt}} = \beta t + T_0 \tag{7}$$

At $t = 0$ the initial conditions are $T(r,z,0) = T_0$ and

Because the thermal conductivity of air is smaller than that of the metal of the cell, we consider that all the energy is transmitted to the plate by the lower boundary of the cell. So, Φ is the sum of the specific heat flow rate through the walls of the metallic cell

$$\Phi = -\frac{1}{M}\sum_i U_i (T_i - T_{\text{plt}}) \Delta A_i \tag{8}$$

where $U_i = U_1$ or U_2.

The finite difference equations are obtained upon integrating Eq. (2) over each of the control volumes. The resulting finite difference scheme at the time $t + \Delta t$ has the following form:

$$a_P T_P = \sum_{nb} a_{nb} T_{nb} + \frac{\rho c_P V_P}{\Delta t} T_P^{\text{old}} + \rho_{ic} \Delta H \frac{V_P}{\Delta t} (X_P - X_P^{\text{old}}) \tag{9}$$

V_P is a volume associated with the Pth node point, the subscripts P, 'nb(E,W,N,S)' and 'old' refer to the Pth node point, the neighboring node points and the old time value, respectively. The calculation of the coefficients a_p and a_{nb} and the resolution of Eq. (9) are presented in Jamil et al. [20] and it is deemed to repeat it in the present work.

3.1. Apparent specific heat capacity

Experimentally, c_p is determined from the equation, $c_p = \delta q/\delta T$, where δq is the specific heat given to (or removed from) the sample at a temperature T, and δT the temperature rise (or decrease) observed. In a frozen PCM, the heat given is consumed in melting solid PCM corresponding to their average melting temperature

$(T+1/2\delta T)$. In this case, the temperature does not rise because the heat absorbed is the latent heat of melting at $(T+1/2\delta T)$. The remaining heat is consumed in raising the temperature of solid PCM and liquid PCM.

$$\delta q = \delta q_{\text{pcm,s}} + \delta q_{\text{pcm,l}} + \delta q_{\text{melting}} \tag{10}$$

where $\delta q_{\text{melting}}$ is the specific heat consumed in melting a fraction solid PCM, $\delta q_{\text{pcm,s}}$ and $\delta q_{\text{pcm,l}}$ are, respectively, the specific heat consumed in raising the temperature of the remaining solid PCM and liquid PCM. Thus the measured c_P:

$$c_p = \left(\frac{\delta q_{\text{pcm,s}} + \delta q_{\text{pcm,l}}}{\delta T}\right) + \frac{m_{\text{pcm,s,melted}}\Delta H}{\delta T} \tag{11}$$

where the product $m_{\text{pcm,s,melted}}\Delta H$ is equal to $\delta q_{\text{melting}}$, and $m_{\text{pcm,s,melted}}$ is (in kg) the liquid PCM formed at an average temperature, $T+1/2\delta T$, on absorption of the heat.

The difference in kilograms of liquid PCM at temperatures, $T+\delta T$ and T, is equal to $m_{\text{pcm,s,melted}}$. In terms of the mass fraction, it is

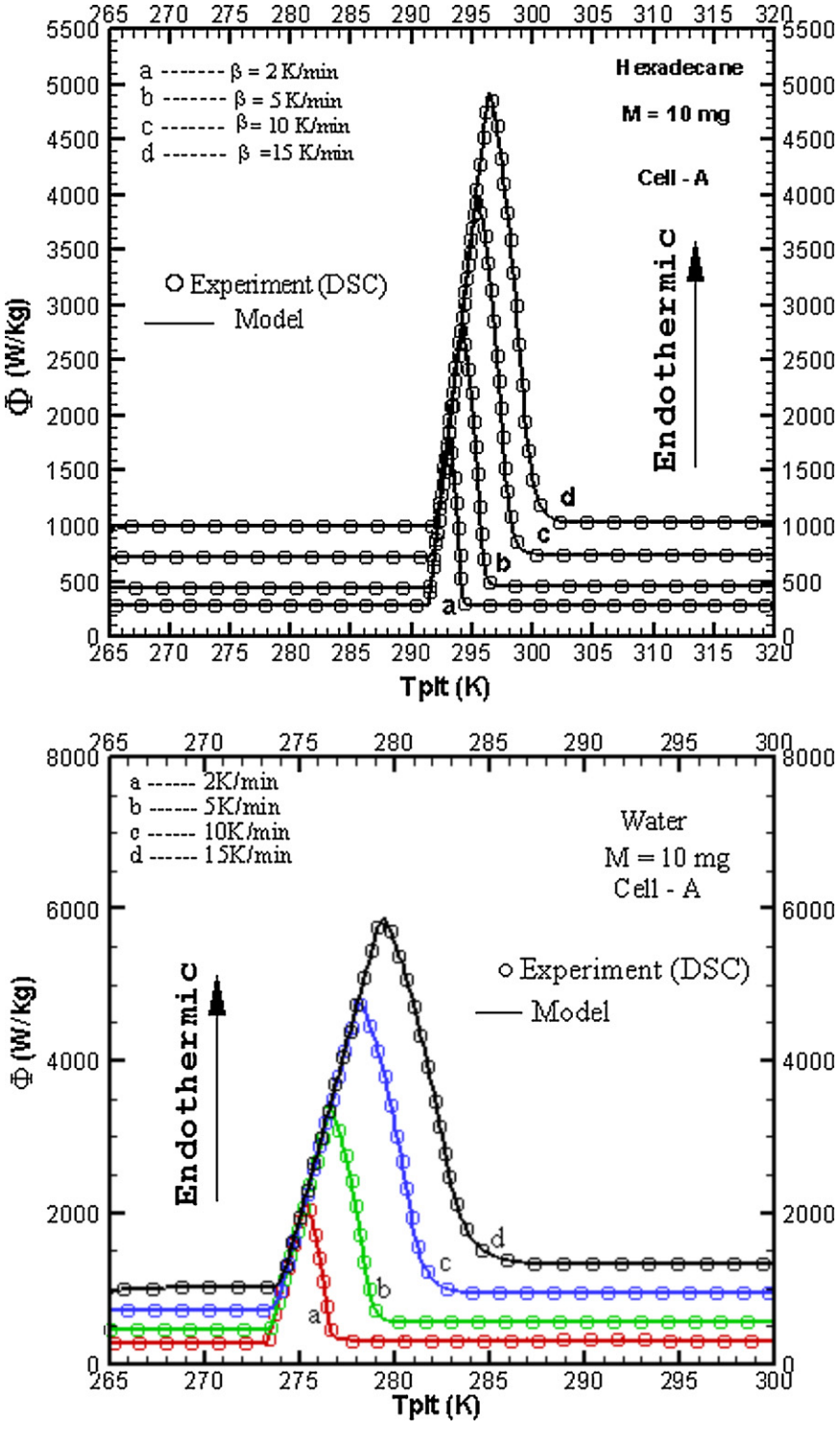

Fig. 2. Effect of the heating rate on the shape of thermograms.

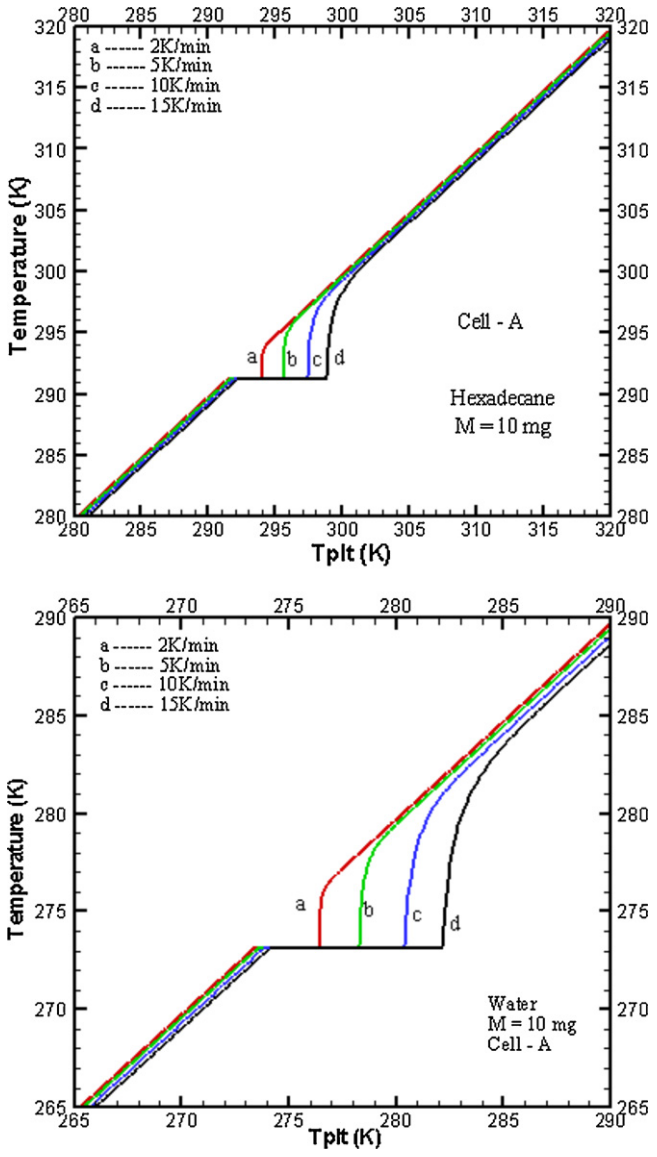

Fig. 3. Influence of the heating rate on the temperature in the centre of the sample.

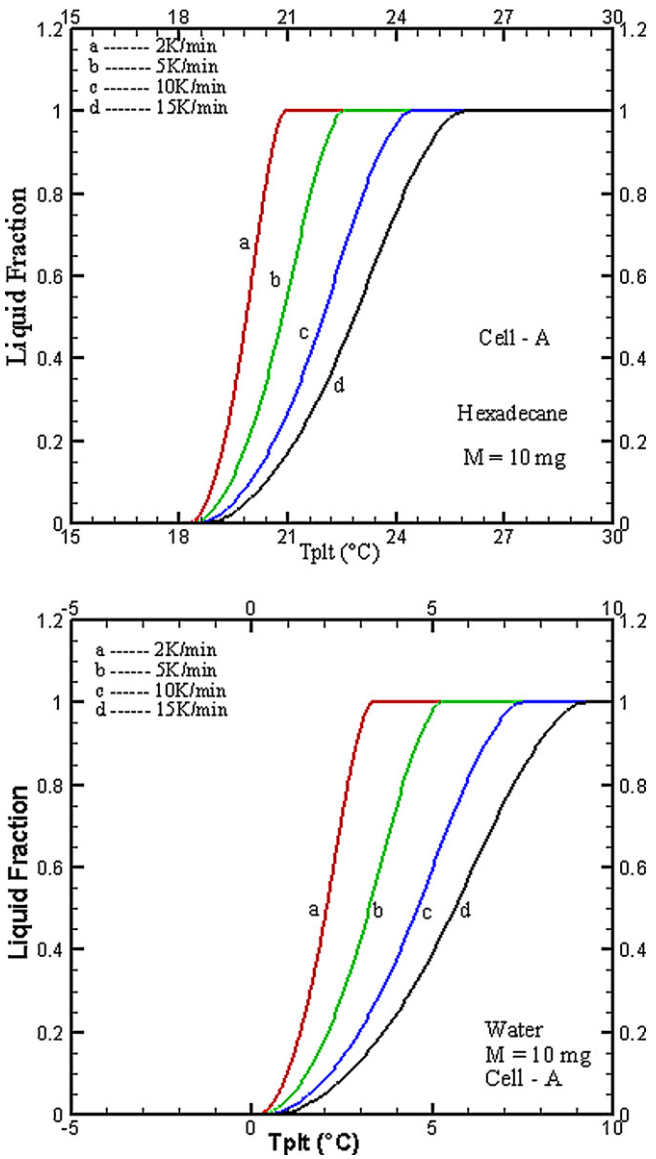

Fig. 4. Liquid fraction for different heating rates.

equal to $[X_{\mathrm{pcm,l},(T+\delta T)} - X_{\mathrm{pcm,l},T}]$ and Eq. (11) becomes:

$$c_p = c_{\mathrm{pcm,s}}(1-X) + c_{\mathrm{pcm,l}}X + \frac{\Delta H[X_{(T+\delta T)} - X_T]}{\delta T} \quad (12)$$

where $c_{\mathrm{pcm,s}}$ and $c_{\mathrm{pcm,l}}$ are, respectively, the heat capacity of solid PCM and liquid PCM at an average temperature $T + 1/2\delta T$.

4. Results and discussion

For the numerical calculation, we have applied the theoretical model described in the previous section. The values of the physical characteristics required in different equations have been determined experimentally or using the literature correlations [1], except the coefficients of heat exchange (U_1 and U_2) that have been determined by simulation from exploratory experiments. In the present work, we present only the numerical results for water and hexadecane.

A comparison of the experimental and numerical curves for various heating rates is given in Fig. 2. Good agreement can be seen in the results. Naturally, no two phase region emerges for and the shape of the thermogram is similar to that for ordinary pure PCM. We note that the melting temperatures range becomes broader and it shifts to greater temperature with increasing heating rate. We can also note that the peak maximum temperature increases continuously which increasing heat rate.

Fig. 3 displays the prediction of the PCM temperature versus the plate temperature T_{plt} at the centre of the sample for different heating rates. It can be seen from this figure that the temperature differences inside the sample become more important as the heating rate increases.

The advantage of the model is that it permits the calculation at each instant the liquid fraction of the PCM inside the cell. During the melting process, the liquid fraction of PCM inside the sample reaches 1 for (hexadecane and water) and this taken as the end point of phase transformation Fig. 4.

From the numerical analysis, we present the specific heat flow rate for different heating rates, as one can see in Fig. 5. The end of the phase change peak in the $c_p(T)$-curve is shifted from 292 K (2 K/min) to about 299 K (15 K/min) for hexadecane and from 273 K (2 K/min) to about 282.5 K (15 K/min) for water. We note that the maximum peak of the $c_p(T)$-curve decreases by increasing the heating rate. These results show clearly that the heating rate is an important factor in determining the thermal behavior of PCM samples in a DSC. In Fig. 6, results of measurements that were done on the

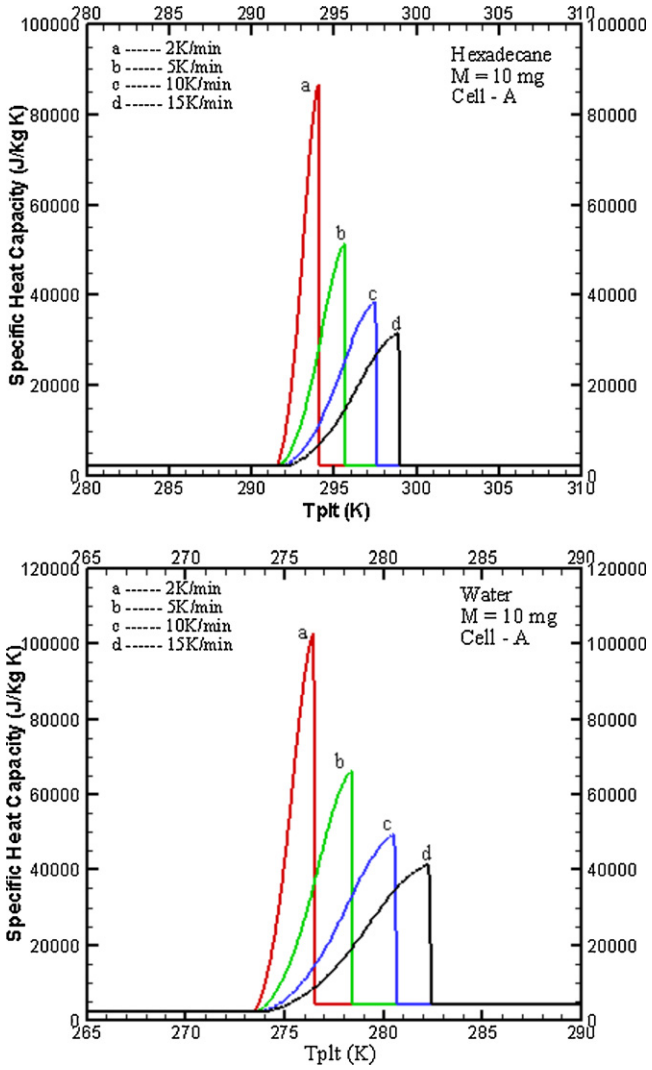

Fig. 5. Effect of the heating rate on the specific heat capacity.

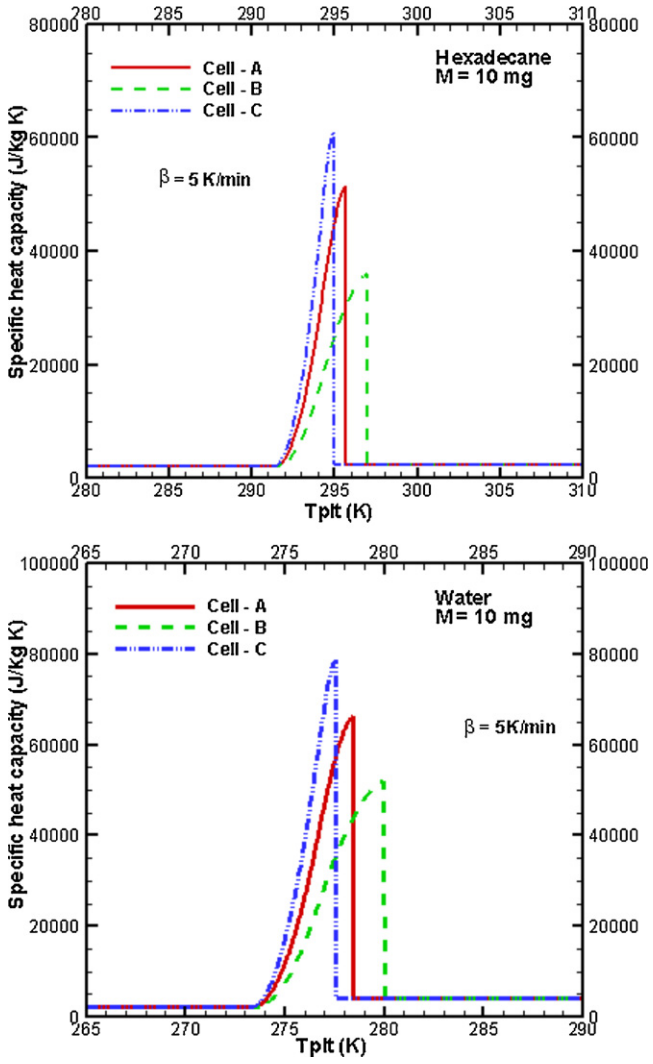

Fig. 6. Effect of the cell geometry on the specific heat capacity.

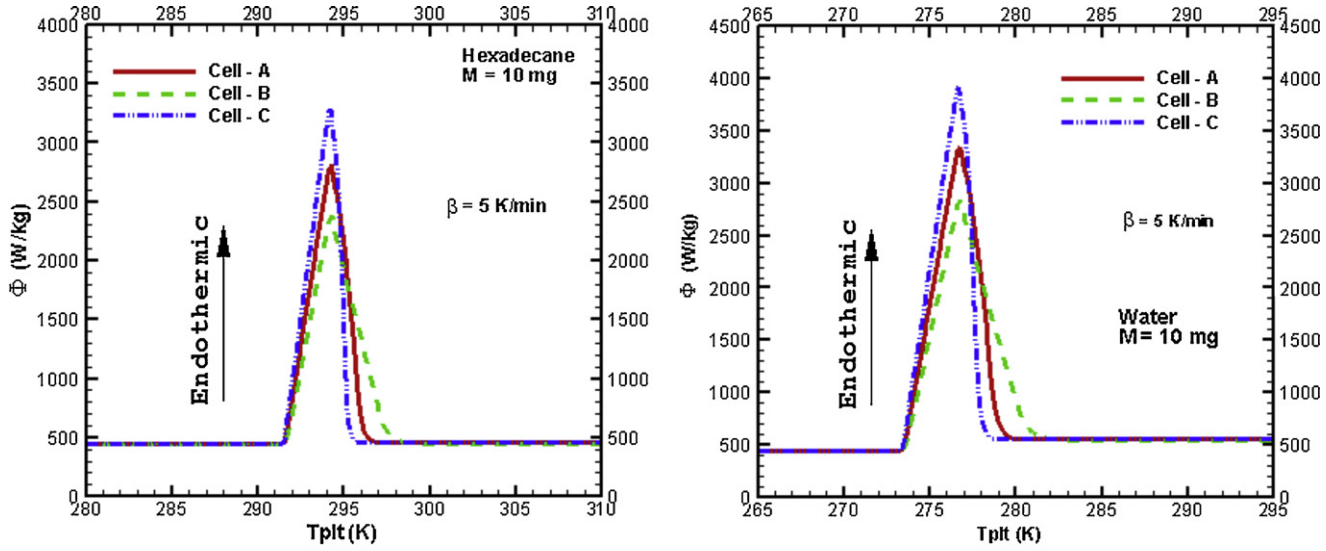

Fig. 7. Effect of the cell geometry on the shape of thermograms.

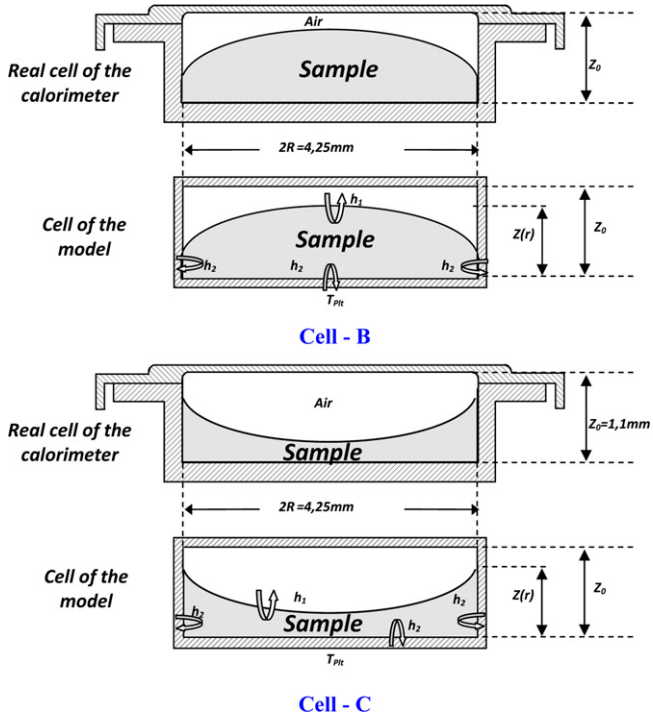

Fig. 8. Cell-B and Cell-C.

same material but with different sample geometries (see Fig. 7) are shown. We note that the end of the phase change peak in the $c_p(T)$-curve is shifted from 295 K (Cell-C) to about 297 K (Cell-B) for hexadecane and from 277.5 K (Cell-C) to about 280 K (Cell-B) for water. It is interesting to note that the area under the sharp peak remains constant (≈335 kJ/kg for water and ≈263 kJ/kg for hexadecane) (see Fig. 8). Again, this as an indication that sample geometry is an important factor in determining the thermal behavior of PCM samples in a DSC. One explanation is that when the phase change process has not completed, any temperature change will lead to a latent heat change and the relation of latent heat change and specific heat capacity with temperature varies with the DSC rate and the sample geometry. To evaluate the specific heat capacity during the melting process, temperature gradient inside the PCM needs to be considered. For a given application that allows for charging/discharging of the storage in a certain temperature range, whether the storage density can reach the value of heat of fusion ΔH, depends on if the allowed temperature range is as large as the phase change temperature range. For designing a PCM thermal energy storage system, storage density, phase change temperatures and specific heat capacity are very important since they decide the storage system's capacity, size and application range. When incorrect phase transition parameters are used in the PCM storage design, it will result in a lower than expected storage capacity.

5. Conclusion

We have examined the influence of the heating rate and the sample geometry on the apparent specific capacity of the PCM during the melting process. It appears from this study that during the melting process both heating rate and PCM geometry affect the DSC thermograms and the apparent specific heat capacity of the PCM.

References

[1] A. Felix Regin, S.C. Solanki, J.S. Saini, Heat storage characteristics of thermal energy storage system using PCM capsules: a review, Renewable and Sustainable Energy Reviews 12 (2008) 2438–2458.
[2] I. Dincer, M.A. Rosen, Energetic, environment and economic aspects of thermal energy storage systems for cooling capacity, Applied Thermal Engineering 21 (2001) 1105–1117.
[3] T. kousksou, F. Strub, J. castaing-Lasvignottes, A. Jamil, J.P. Bédécarrats, Second law analysis of latent thermal storage for solar system, Solar Energy Materials and Solar Cells 91 (2007) 1275–1281.
[4] A. Abhat, Low temperature latent heat thermal energy storage: heat storage materials, Solar Energy 30 (1983) 313–332.
[5] S.M. Husnain, Review on sustainable thermal energy storage technologies. 1. Heat storage materials and techniques, Energy Conversion and Management 39 (1998) 1127–1138.
[6] I. Dincer, Thermal Energy Storage: Systems and Applications, John Wiley & Sons, 2002.
[7] M.F. Mohammed, M.K. Amar, A.K.R. Siddique, A.H. Said, A review on phase change energy storage: materials and applications, Energy Conversion and Management 45 (2004) 1597–1615.
[8] B. Zalba, J.M. Martin, L.F. Cabeza, H. Mehling, Review on thermal energy storage with phase change: materials, heat transfer analysis and applications, Applied Thermal Engineering 23 (2003) 251–283.
[9] T. Kousksou, A. Jamil, Y. Zeraouli, J.P. Dumas, Equilibrium liquidus temperatures of binary mixtures from differential scanning calorimetry, Chemical Engineering Science 62 (2007) 6516–6523.
[10] G.W.H. Hohne, W. Hemminger, H.J. Flammersheim, Differential Scanning Calorimetry, Springer–Verlag, Berlin, 1996.
[11] W. Hemminger, G. Hohne, Calorimetry Fundamentals and Practice, Verlag, Weinheim, 1984.
[12] M. Merzlyakov, C. Schick, Thermal conductivity from dynamic response of DSC, Thermochimica Acta 377 (2001) 183–191.
[13] C. Dalmazzone, C. Noik, D. Clausse, Oil & Gas Science and Technology: Review IFP (2008).
[14] A. Jamil, T. Kousksou, K. El Omari, Y. Zeraouli, Y. Le Guer, Heat transfer in salt solutions enclosed in DSC cells, Thermochimica Acta 507–508 (2010) 15–20.
[15] M.J. Richardson, Quantitative aspects of differential scanning calorimetry, Thermochimica Acta 300 (1997) 15–28.
[16] S. Rudtsch, Uncertainty of heat capacity measurements with differential scanning calorimeters, Thermochimica Acta 382 (2002) 17–25.
[17] T. Kousksou, A. Jamil, Y. Zeraouli, J.-P. Dumas, DSC study and computer modeling of the melting process in ice slurry, Thermochimica Acta 448 (2006) 123–129.
[18] V.R. Voller, Implicit finite-difference solutions of the enthalpy formulation of Stefan problems, IMA Journal of Numerical Analysis 5 (1985) 201–214.
[19] V. Voller, C.R. Swaminathan, General source-based method for solidification phase change, Numerical Heat Transfer B 19 (1991) 175–189.
[20] A. Jamil, T. Kousksou, Y. Zeraouli, S. Gibout, J.-P. Dumas, Simulation of the thermal transfer during an eutectic melting of a binary solution, Thermochimica Acta 441 (2006) 30–34.